Journal of Materials Chemistry A

Accepted Manuscript

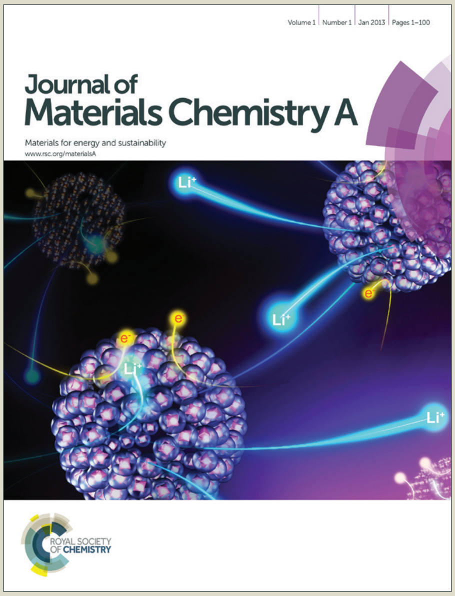

ROYAL SOCIETY OF CHEMISTRY

www.rsc.org/materialsA

Energy & Environmental Science RSCPublishing

COMMUNICATION

Cite this: DOI: 10.1039/x0xx00000x

Low-Bandgap Thieno[3,4-*c*]pyrrole-4,6-dione-Polymers for High-performance Solar Cells with Significantly Enhanced Photocurrents

Received 00th January 2015,
Accepted 00th January 2015

DOI: 10.1039/x0xx00000x

www.rsc.org/

Cheng Zhang,[a] Hui Li,[a] Jizheng Wang,[a] Yongfang Zhang,[a] Yan Qiao,[c] Dazhen Huang,[a] Chong-an Di,[a] Xiaowei Zhan,[b] Xiaozhang Zhu*[a] and Daoben Zhu[a]

Low-bandgap thieno[3,4-*c*]pyrrole-4,6-dione-polymers with proximal and distal configurations were synthesized for polymer solar cells. Photovoltaic performance depends on the orientation of the fused thiophene subunits, which is related to the different semiconducting property and phase separation. Without special device treatments, P3 showed power conversion efficiencies of up to 7.50% with the highest short-circuit current (J_{sc} = 18.2 mA/cm^2) so far reported for TPD polymers.

During the last decade, conjugated copolymers designed with alternating donor/acceptor (D/A) or quinoid (D-Q, Q: quinoid-enhancing moieties) approaches have been intensively explored, leading to substantial progresses in the field of polymer solar cells (PSCs).[1] Several mid-bandgap (MBG) copolymers[2] with typical optical bandgaps (E_g^{opt}) of approximately 1.7 eV have delivered promising power conversion efficiencies (PCEs) of over 8% in a conventional device structure.[3] Further increasing the PCEs requires the development of low-bandgap (LBG) polymers with E_g^{opt} of approximately 1.5 eV for utilizing solar energy in the near-infrared (near-IR) region.[4] Thus far, the development of high-performance LBG-type polymers lags behind that of MBG polymers, and 2,5-dialkyl-pyrrolo[3,4-*c*]pyrrole-1,4-dione (DPP)-containing polymers are representative LBG polymers because of the strong electron-withdrawing ability of the DPP acceptor.[5] The development of LBG-polymers with optimized electronic energy levels is currently enslaved to the scarcity of effective acceptor units just like DPP.[6]

The thieno[3,4-*c*]pyrrole-4,6-dione (TPD) motif[7] is viewed as one of the most valuable electron-deficient moieties available for the construction of MBG-polymers (E_g^{opt}: ca. 1.8 eV), by copolymerization with weakly electron-donating benzo[1,2-*b*:4,5-*b'*]dithiophene (BDT),[8] giving high PCEs of up to 8.5% with moderate J_{sc} of approximately 12.6 mA/cm^2.[3a] Because of the less electron-deficient property of TPD than of DPP, LBG TPD-polymers were rarely studied, which, however, is important for further enhancing J_{sc} and may result in better photovoltaic performance.[7,3a] The incorporation of electron-rich moieties, such as *N*-alkyl-dithieno[3,2-*b*:2',3'-*d*]pyrrole (DTP), reduces the optical bandgaps of TPD polymers to 1.59 eV, but leads to even lower PCE (1.69% and J_{sc}=4.69 mA/cm^2).[9] Novel acceptor combinations consisting of two TPDs or TPD with other acceptor units were also developed by Leclerc et. al. for modulating energy levels.[10] By regioselectively inserting TT, an important moiety used in quinoid strategy,[11] into BDT (donor) and TPD (acceptor) units, we designed two kinds of TPD polymers with low E_g^{opt} of approximately 1.5 eV, PBDT$_{TEH}$-TBTT$_{EH}$-*i* (**P1**) and PBDT$_{TEH}$-TBTT$_{EH}$-*o* (**P2**) with different regiochemical feature (Fig. 1). TBTTs, TPD flanked with two unsymmetrical TT moieties regioselectively, are the key π-building blocks for the construction of **P1**–**P3** and are reported by us for high-performance n-type organic semiconductors.[12] We found that the PSC performance was sensitive to the orientation of the fused thiophene units, with maximum PCEs of 6.06% (**P1**) vs. 4.21% (**P2**) under optimized conditions in a conventional device setup, which can be attributed to the inferior phase separation and carrier transporting ability of **P2**. The inverted device based on **P1** furnished short-circuit current (J_{sc}) up to 18 mA/cm^2, resulting in a higher PCE of 6.70%. Given that the aliphatic side chains usually play a vital role in device performance,[3a,13] we explored the use of **P3**, with 2-hexyldecyl (HD) group on TPD unit, and found that this polymer could be used to further tune the thin-film morphology and afford PCEs of up to 7.50% without additive and thermal annealing, which favors the need of industrially producing OSC materials.

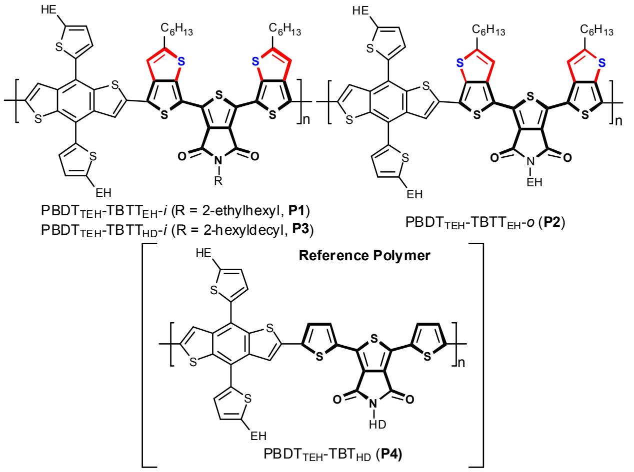

Fig. 1 Molecular structures of TBTT-based polymers.

TBTTs were synthesized according to our reported method.[12] The maximum absorptions of TBTTs were markedly bathochromically shifted compared with those of TBT (ca. 70 nm), with smaller stokes shift of 1926 (TBTT-*i*) and 2906 cm^{-1} (TBTT-*o*) vs. 4160 cm^{-1} (TBT, TPD flanked with two thiophene units) (Fig. S1). In addition to the weak O–S intramolecular interactions,[14] the additional short S–S contacts in TBTT-*i* can also contribute to its planar conformation. Compared with TBTT-*o*, the structural absorption and smaller Stokes shift of TBTT-*i* suggest that it has a more rigid conformation, which can be clearly deduced from the theoretical calculations at the B3LYP/6-31G** level. While TBTT-*i* is fully coplanar, TBTT-*o* shows a twisted structure with a dihedral angle of 14.8° (Fig. S2).

Polymers with different thiophene orientations, **P1**, **P2**, and **P3**,[15] were synthesized by standard Pd-catalyzed Stille reaction and were purified by Soxhlet extraction with methanol, hexane, and either chloroform or chlorobenzene, successively. The key TBTT$_{EH}$-2Br π-building blocks were synthesized according to our previously reported procedures.[12] The number-average molecular weight (M$_n$) and polydispersity (PDI) of **P1**–**P3** are 7.93, 5.52, and 6.07 KDa, and 4.21, 3.98, and 3.77, respectively, which were estimated by gel-permeation chromatography (GPC) at 150 °C using 1,2,4-trichlorobenzene as the eluent.[16] These polymers showed good solubility in *o*-dichlorobenzene (>10 mg/mL) and excellent thermal stability (up to 390, 400, and 355 °C, respectively, at which 5wt% loss was recorded, Fig. S6). As indicated in Fig. 2 and Fig. S3, compared with the reference polymer, PBDT$_{TEH}$-TBT$_{HD}$ (**P4**: λ_{max}^{abs}: 596 nm), **P1**–**P3** exhibited near-IR absorption (λ_{max}^{abs}: 726, 706, and 725 nm, respectively) with bathochromic shifts of over 100 nm, which indicates that the incorporation of thiophene unit cannot alter the MBG nature of PBDT-TPD-polymers, and the LBG nature of **P1**–**P3** is endowed by quinoid-enhancing ability of TT.[7a] In contrast to **P2**, polymers **P1** and **P3** exhibited absorptions with obvious aggregation peaks, implying their more ordered packing in thin films. The optical bandgaps of **P1**–**P3** were 1.54, 1.46, and 1.56 eV, respectively, which are significantly narrower than that of **P4** (1.88 eV) by approximately 0.30 eV. The HOMO (highest occupied molecular orbital) energy levels of the polymers were determined to be −4.64 eV (**P1**), −4.63 eV (**P2**), and −4.78 eV (**P3**) by ultroviolet photoelectron spectroscopy (UPS) of polymer thin films on silicon wafer (Fig. S5).

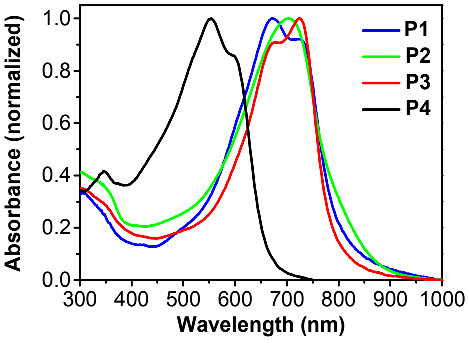

Fig. 2 UV-Vis-NIR absorption spectra of **P1** (blue), **P2** (green), **P3** (red), and **P4** (black) in thin films spun from *o*-dichlorobenzene solution.

We first investigated the photovoltaic performances of **P1** and **P2** with conventional BHJ device configuration, ITO/PEDOT:PSS/polymers:PC$_{71}$BM/Ca/Al, which were tested under simulated 100 mW/cm^2 AM 1.5G illumination; the results are summarized in Table 1. The active layer was formed by spin-coating with an *o*-dichlorobenzene (*o*-DCB) solution of polymer:PC$_{71}$BM (1:1 weight ratio, 10 mg/mL). As shown in Table 1, PCE values of up to 5.71% were obtained from the **P1**-based PSCs with thermal annealing of the blend films. Finally, 3% (v/v) 1,8-diiodooctane (DIO) was utilized as an additional processing additive, giving PCE values of 6.06 (**P1**) and 4.21% (**P2**). Further device optimization of **P1** and **P2** was undertaken with the inverted device geometry (ITO/ZnO/polymers:PC$_{71}$BM/MoO$_3$/Ag), which can provide better device stability due to the absence of corrosive PEDOT:PSS hole transporting layer and low work function cathode. As shown in Fig 3., the inverted devices gave promising PCEs of up to 6.70% with further improved J_{sc} values close to 17.77 mA/cm^2 and 4.45%.[17] High external quantum efficiencies (EQEs) of **P1** over 60% between a wide range of wavelengths (420–760 nm, with a peak value of 75% at 680 nm) were also recorded, with the responsive tail approaching approximately 850 nm, which is consistent with the absorption spectra. The high EQEs are consistent with large J_{sc} values (ca. 3% error). By contrast, the EQE responsive tail of the best MBG TPD polymers,[3a] PBDTTPDs, reach approximately 700 nm, leading to a lower J_{sc} of 12.6 mA/cm^2. The enhanced J_{sc} of **P1** can be unambiguously attributed to its intrinsic LBG nature.

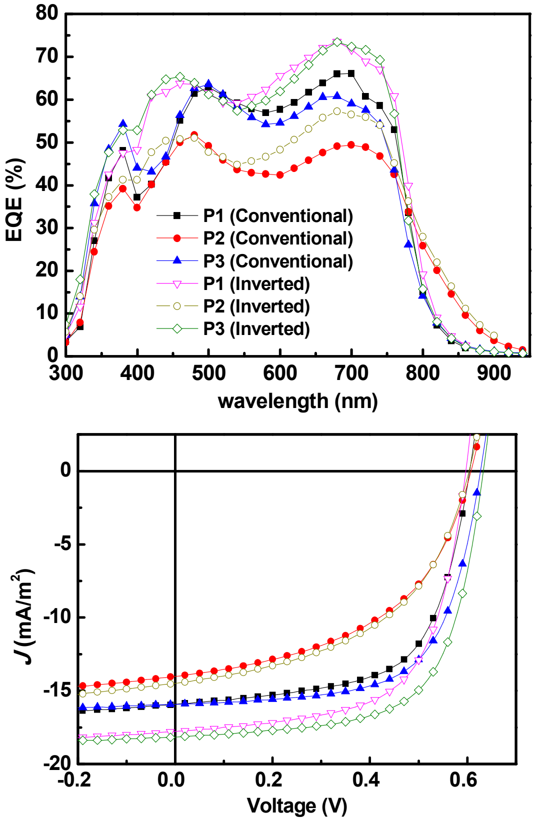

Fig. 3 EQE (top) and *J-V* (bottom) curves of the optimized conventional and inverted solar cell devices based on **P1**–**P3**.

The disparate device performance of **P1** and **P2** is a fascinating issue, and a detailed examination of the origins of this difference could further clarify the relationship between molecular structure and device performance. By analyzing in detail the device parameters of **P1** and **P2** reported in Table 1, we found that both polymers gave similar open-circuit voltage (V_{oc}) values of approximately 0.6 V, which is consistent with their similar HOMO energy levels. However, although **P2** can absorb slightly more light in the near-IR region than can **P1**, as indicated in Fig 2, J_{sc} and fill factors (FF) values of **P2** (15.21 mA/cm^2, 48.58%) were inferior to those of **P1** (17.77 mA/cm^2, 63.13%). The carrier mobilities of both compounds in pristine films were examined by the field-effect transistor (FET) method. We found that **P1** showed excellent hole-transporting mobility of 0.15 cm^2 V^{-1} s^{-1}, which is higher than that of **P2** (0.017 cm^2 V^{-1} s^{-1}) by nearly one order of magnitude (Fig. S12), which might be correlated with the different degree of planarity of the TBTTs.[18] Given that the pristine mobility does not always represent the carrier-transporting ability in blend active layers of OPV devices, we further examined the carrier mobilities of the blend films that were prepared under the same conditions used for the optimized devices by applying the space-charge-limited current (SCLC) method. The blend films of both polymers showed balanced hole and electron mobilities, 3.96×10^{-4} cm^2 V^{-1} s^{-1} (μ_h), 1.28×10^{-4} cm^2 V^{-1} s^{-1} (μ_e) for **P1** and 3.57×10^{-5} cm^2 V^{-1} s^{-1} (μ_h), 4.63×10^{-5} cm^2 V^{-1} s^{-1} (μ_e) for **P2**. Thus, both measuring methods point to the better semiconducting properties of **P1** compared with that of **P2**. We consider that the larger J_{sc} values of **P1** may result from more favorable charge transport. The morphology of the active layer[19] is another key factor that can affect device performance significantly. X-ray diffraction (XRD) measurements (Fig. S8) revealed the amorphous nature of the polymer:PC$_{71}$BM blends. The polymer:PC$_{71}$BM blend films of the best device conditions were also investigated by atomic force microscopy (AFM) and transmission electron microscopy (TEM). As shown in Fig. S9, **P1**:PC$_{71}$BM blend film is much rougher than **P2**:PC$_{71}$BM blend film, giving a root-mean-square (RMS) surface roughness of 4.16 nm. Comparatively, **P2**:PC$_{71}$BM blend film only gives a RMS value of 1.43 nm. Also, the domains shown **P1**:PC$_{71}$BM film are more distinct than that in **P2**:PC$_{71}$BM film, implying better phase separation. Similar differences are also observed in AFM phase images and TEM images for the two films. According to the above discussion, **P1** and **P2** with different orientation of fused thiophene units on the TBTT building blocks show significantly different photovoltaic performance, which may be related to varied semiconductiviy and film morphology. This highlights the importance of incorporating specific structural regularity[20] in the rational design of conjugated polymers, and also reveals the complexity of predicting material performance.[12]

Given that the nature of the side alkyl chains plays a key role in the self-assembling properties of the polymer and the resulting device performance,[3a,13] we evaluated the suitability of polymer **P3**, with longer branched 2-hexyldecyl (HD) chain, in device construction. To our surprise, a higher PCE of 6.47% was obtained with conventional device configuration. Even higher PCE values of up to 7.50% could be readily achieved with inverted device configuration without the use of additional post-treatment and/or additives.[21] Compared with **P2**, polymer **P3** comprehensively promoted all three parameters that determine the PCE, and the TEM images show a slight little phase separation scale (~130 nm) than that of **P1**:PC$_{71}$BM blends (~150 nm), which may explain the larger J_{sc} and FF of **P3**:PC$_{71}$BM blend films with the easier charge separation and charge transport. (Fig. S10). More balanced hole and electron mobilities are also observed in the optimized **P3**:PC$_{71}$BM blend film, 1.44×10^{-4} cm^2 V^{-1} s^{-1} (μ_h) and 1.79×10^{-4} cm^2 V^{-1} s^{-1} (μ_e). Given that **P1**–**P3** are the first three examples of this series, we optimistically expect that TBTT-based LBG-polymers will be suitable for the development of high-performance solar cells by further optimizing the molecular system especially via lowering HOMO energy levels[22] and device engineering.

So far, high-performance TPD polymers have an exclusively common structural feature that the TPD units are substituted with linear alkyl chains.[7] McGehee et. al. demonstrated that this structural feature was favorable for the close contact between fullerene and TPD moiety of polymers.[23] Thus, it is an exceptive example among TPD copolymers that **P1**–**P3** with branched alkyl chains on TPDs can work well in PSCs. Taking close inspection on the molecular structures of **P1**–**P3**, we deduce that 2D-expanded π-surfaces of TBTTs can reduce the negative effect of branched alkyl chains on TPD, meanwhile enhance the fullerene-TBTT approaching. The geometry sizes of optimized TBTT structures (Fig. S1) are approximately 10 Å in length and 7 Å in width, which is suitable for seating one PC$_{71}$BM molecule. Accordingly, we found that the TBTT (acceptor) moieties of **P1** showed 2D correlations with the pendant ester groups of PC$_{61}$BM as deduced from the solid-state 2D ^{13}C{^{1}H} HETCOR NMR measurements of **P1**:PC$_{61}$BM blend.[24]

Table 1 Photovoltaic Performance of the TBTT polymers in conventional[a] and inverted[b] BHJ Devices with PC$_{71}$BM.

polymer	DIO[c]	V_{oc} [V]	J_{sc} [mA/cm^2]	FF [%]	PCE [%][f]
P1	N	0.619	14.14	59.82	5.26 [5.09][a]
	N[d]	0.622	14.71	62.43	5.21 [5.46][a]
	Y[d]	0.605	15.92	62.92	6.06 [5.91][a]
	N[d]	0.618	16.44	62.16	6.32 [6.16][b]
	Y[d]	0.597	17.77	63.13	6.70 [6.48][b]
P2	N	0.587	11.73	42.92	2.95 [2.84][b]
	N[d]	0.608	12.20	47.86	3.55 [3.40][a]
	Y[d]	0.607	14.02	49.51	4.21 [4.01][a]
	Y[d]	0.603	15.21	48.58	4.45 [4.37][b]
P3	N	0.627	15.93	64.76	6.47 [6.23][a,e]
	N	0.633	18.15	65.20	7.50 [7.32][b,e]

[a] Structure of ITO/PEDOT:PSS/Polymers:PC$_{71}$BM (1:1 weight ratio)/Ca/Al; [b] Inverted structure of ITO/ZnO/Polymers:PC$_{71}$BM (1:1 weight ratio)/MoO$_3$/Ag; [c] Devices were fabricated from blend without (N) or with (Y) 3% (v/v) DIO as a processing additive; [d] Thermal annealing. [e] Polymer:PC$_{71}$BM (1:1.5 weight ratio); [f] The values in square brackets indicate the average values of PCEs obtained from more than twenty devices.

In summary, we have successfully developed TPD-type LBG-polymers combining two classical approaches to polymer design: D-A and quinoid strategies.[25] This D-Q-A-Q arrangement endowed TPD polymers with low optical bandgap and favorable charge-separation property deriving from the enhanced quinoidal resonance and the short-distance contact between fullerene and 2D TBTT respectively. The use of TPDs substituted with branched alkyl chains may enhance the solution processability of the polymers, but has no negative effect on device performance. Low bandgaps do not always guarantee high J_{sc}, however, inverted PSC devices with **P3**:PC$_{71}$BM blend films show promising J_{sc} of up to 18.2 mA/cm^2 with PCE values of up to 7.50% without requiring additional device treatment or additives, which is among the best reported for LBG-polymers to date. We expect that LBG-polymers designed by inserting quinoid-enhancing moiety into D-A polymers will lead to high-performance single-junction or tandem solar cells.[26]

Acknowledgements

We thank the National Basic Research Program of China (973 Program) (No. 2014CB643502), the Strategic Priority Research Program of the Chinese Academy of Sciences (XDB12010200), and the National Natural Science Foundation of China (91333113) for financial support.

Notes and references

Cheng Zhang and Hui Li contributed equally.

[a] *Beijing National Laboratory for Molecular Sciences, CAS Key Laboratory of Organic Solids, Institute of Chemistry, Chinese Academy of Sciences, Beijing, China. Fax: +86-10-82449133; Tel: +86-10-82449133; E-mail: xzzhu@iccas.ac.cn*

[b] *Department of Materials Science and Engineering, College of Engineering, Peking University, Beijing 100871, P. R. China.*

[c] *State Key Laboratory of Coal Conversion, Institute of Coal Chemistry, Chinese Academy of Sciences, Taiyuan, Shanxi Province, 030001, P. R. China.*

† Electronic Supplementary Information (ESI) available: synthetic details, polymer characterizations, and details concerning OFET and PSC device fabrication and characterization. See DOI: 10.1039/c000000x/

1 (a) L. Dou, J. You, Z. Hong, Z. Xu, G. Li, R. A. Street and Y. Yang, *Adv. Mater.*, 2013, **46**, 6642; b) F. He and L. Yu, *J. Phys. Chem. Lett.*, 2011, **2**, 3102; (c) C. J. Brabec, S. Gowrisanker, J. J. M. Hall, D. Laird, S. Jia and S. P. Williams, *Adv. Mater.*, 2010, **22**, 3839; (d) Z.-G. Zhang and J. Wang, *J. Mater. Chem.*, 2012, **22**, 4178; (e) B. C. Thompson and J. M. J. Fréchet, *Angew. Chem., Int. Ed.*, 2007, **47**, 58.

2 The concept of MBG-polymers was defined by Yang et. al. in the following paper: L. Dou, W.-H. Chang, J. Gao, C.-C. Chen, J. You and Y. Yang, *Adv. Mater.*, 2013, **25**, 825.

3 (a) C. Cabanetos, A. E. Labban, J. A. Bartelt, J. D. Douglas, W. R. Mateker, J. M. L. Fréchet, M. D. McGehee and P. M. Beaujuge, *J. Am. Chem. Soc.*, 2013, **135**, 4656; (b) M. Zhang, Y. Gu, X. Guo, F. Liu, S. Zhang, L. Huo, T. P. Russell and J. Hou, *Adv. Mater.*, 2013, **25**, 4944; (c) N. Wang, Z. Chen, W. Wei and Z. Jiang *J. Am. Chem. Soc.*, 2013, **135**, 17060; (d) I. Osaka, T. Kakara, N. Takemura, T. Koganezawa and K. Takimiya, *J. Am. Chem. Soc.*, 2013, **135**, 8834.

4 M. C. Scharber, D. Mühlbacher, M. Koppe, P. Denk, C. Waldauf, A. J. Heeger and C. Brabec, *Adv. Mater.*, 2006, **18**, 789.

5 (a) M. M. Wienk, M. Turbiez, J. Gilot and R. A. J. Janssen, *Adv. Mater.*, 2008, **20**, 2556; b) J. C. Bijleveld, A. P. Zoombelt, S. G. J. Mathijssen, M. M. Wienk, M. Turbiez, D. M. de Leeuw and R. A. J. Janssen, *J. Am. Chem. Soc.*, 2009, **131**, 16616; (c) K. H. Hendriks, G. L. Heintages, V. S. Gevaerts, M. M. Wienk and R. A. J. Janssen, *Angew. Chem., Int. Ed.*, 2013, **52**, 8341; (d) L. Dou, J. Gao, E. Richard, J. You, C.-C. Chen, K. C. Cha, Y. He, G. Li and Y. Yang, *J. Am. Chem. Soc.*, 2012, **134**, 10071; (e) Y. Li, P. Sonar, L. Murphy and W. Hong, *Energy Environ. Sci.*, 2013, **6**, 1684. Selected other examples: (a) L. Dou, C.-C. Chen, K. Yoshimura, K. Ohya, W.-H. Chang, J. Gao, Y. Liu, E. Richard and Y. Yang, *Macromolecules*, 2013, **46**, 3384; (b) H. Zhou, L. Yang, S. C. Price, K. J. Knight and W. You, *Angew. Chem., Int. Ed.*, 2010, **49**, 7992; (c) D. Mühlbacher, M. Scharber, M. Morana, Z. Zhu, D. Waller, R. Gaudiana and C. Brabec, *Adv. Mater.*, 2006, **18**, 2884.

6 J. D. Yuen, and F. Wudl, *Energy Environ Sci.*, 2013, **6**, 392.

7 (a) A. Pron, P. Berrouard and M. Leclerc, *Macromol. Chem. Phys.*, 2013, **214**, 7; (b) Y. Zou, A. Najari, P. Berrouard, S. Beaupré, R. A. Badrou, Y. Tao and M. Leclerc, *J. Am. Chem. Soc.*, 2010, **132**, 5330; (c) C. Piliego, T. W. Holcombe, J. D. Douglas, C. H. Woo, P. M. Beaujuge and J. M. J. Fréchet, *J. Am. Chem. Soc.*, 2010, **132**, 7595; (d) H. Zhong, F. Deledalle, E. C. Fregoso, M. Shahid, Z. Fei, C. B. Nielsen, N. Yaacobi-Gross, S. Rossbauer, T. D. Anthopoulos, J. R. Durrant and M. Heeney, *J. Am. Chem. Soc.*, 2013, **135**, 2040; (e) T.-Y. Chu, J. Lu, S. Beaupé, Y. Zhang, J. R. Pouliot, S. Wakim, J. Zhou, M. Leclerc, Z. Li, J. Ding and Y. Tao, *J. Am. Chem. Soc.*, 2011, **133**, 4250. (f) Z. Li, S. Tsang, X. Du, L. Scoles, G. Robertson, Y. Zhang, F. Toll, Y. Tao, J. Lu and J. Ding, *Adv. Funct. Mater.*, 2011, **21**, 3331.

8 L. Huo and J. Hou, *Poly. Chem.*, 2011, **2**, 2453.

9 Y. Zhang, J. Zou, H.-L. Yip, Y. Sun, J. A. Davies, K.-S. Chen, O. Acton and A. K.-Y. Jen, *J. Mater. Chem.*, 2011, **21**, 3895.

10 (a) J.-R. Pouliot, L. G. Mercier, S. Caron and M. Leclerc, *Macromol. Chem. Phys.*, 2013, **214**, 453; (b) F. Grenier, P. Berrouard, J.-R. Pouliot, H.-R. Tseng, A. J. Heeger and M. Leclerc, *Polym. Chem.*, 2013, **4**, 1836; (c) C. Ottone, P. Berrouard, G. Louarn, S. Beaupré, D. Gendron, M. Zagorska, P.; Rannou, A. Najari, S. Sadki, M. Leclerc and A. Pron, *Polym. Chem.*, 2012, **3**, 2355; (d) P. Berrouard, F. Grenier, J.-R. Pouliot; E. Gagnon, C. Tessier and M. Leclerc, *Org. Lett.*, 2010, **13**, 38.

11 (a) Y. Liang and L. Yu, *Acc. Chem. Res.*, 2010, **43**, 1227; (b) L. Lu and L. Yu, *Adv. Mater.*, 2014, **26**, 4413.

12 C. Zhang, Y. Zang, E. Gann, C. R. McNeill, X. Zhu, C.-a. Di and D. Zhu, *J. Am. Chem. Soc.*, 2014, **136**, 16176.

13 (a) T. Lei, J.-Y. Wang and J. Pei, *Chem. Mater.*, 2014, **26**, 594; (b) J. Mei and Z. Bao, *Chem. Mater.*, 2014, **26**, 604; (c) I. Meager, R. S. Ashraf, S. Mollinger, B. C. Schroeder, H. Bronstein, D. Beatrup, M. S. Vezie, T. Kirchartz, A. Salleo, J. Nelson and I. McCulloch, *J. Am. Chem. Soc.*, 2013, **135**, 11537; (d) B. C. Thompson, B. J. Kim, D. F. Kavulak, K. Sivula, C. Mauldin and J. M. J. Fréchet, *Macromolecules*, 2007, **40**, 7425; (e) W. Li, K. H. Hendriks, A. Furlan, W. S. C. Roelofs, S. C. J. Meskers, M. M. Wienk and R. A. J. Janssen, *Adv. Mater.*, 2014, **26**, 1565.

14 (a) N. E. Jackson, B. M. Savoie, K. L. Kohlstedt, M. O. de la Cruz, G. C. Schatz, L. X. Chen and M. A. Ratner, *J. Am. Chem. Soc.*, 2013, **135**, 10475; (b) X. Guo, N. Zhou, S. J. Lou, J. W. Hennek, R. P. Ortiz, M. R. Butler, P.-L. T. Boudreault, J. Strzalka, P.-O. Morin, M. Leclerc, J. T. L. Navarrete, M. A. Ratner, L. X. Chen, R. P. H. Chang, A. Facchetti and T. J. Marks, *J. Am. Chem. Soc.*, 2012, **134**, 18427; (c) J.-F. Jheng, Y.-Y. Lai, J.-S. Wu, Y.-H. Chao, C.-L. Wang and C.-S. Hsu, *Adv. Mater.*, 2013, **25**, 2445; (d) X. Guo, J. Quinn, Z. Chen, H. Usta, Y. Zheng, Y. Xia, J. W. Hennek, R. P. Ortiz, T. J. Marks and A. Facchetti, *J. Am. Chem. Soc.*, 2013, **135**, 1986.

15 Polymers with linear alkyl chains on TPDs showed too low solubility to fabricate reasonable photovoltaic devices.

16 Under the same condition, we got a low number average molecular weight of 26.6 kDa and polydispersity of 2.1 for commercial P3HT (Mn: 50 kDa, PDI: 1.7).

17 Z. Xu, L.-M. Chem, G. Yang, C.-H. Huang, J. Hou, Y. Wu, G. Li, C.-S. Hsu and Y. Yang, *Adv. Funct. Mater.*, 2009, **19**, 1227.

18 T. Lei, X. Xia, J.-Y. Wang, C.-J. Liu and J. Pei, *J. Am. Chem. Soc.*, 2014, **136**, 2135.

19 Y. Huang, E. J. Kramer, A. J. Heeger and G. C. Bazan, *Chem. Rev.*, 2014, 114, 7006.

20 (a) N. E. Jackson, B. M. Savoie, K. L. Kohlstedt, T. J. Marks, L. X. Chen and M. A. Ratner, *Macromolecules*, 2014, **47**, 987; (b) G. C. Welch, R. C. Bakus, S. J. Teat and G. C. Bazan, *J. Am. Chem. Soc.*, 2013, **135**, 2298; (c) M. Wang, H. Wang, T. Yokoyama, X. Liu, Y.

Huang, Y. Zhang, T.-Q. Nguyen, S. Aramaki and G. C. Bazan, *J. Am. Chem. Soc.*, 2014, **136**, 12576.

21 The thermal annealing or use of DIO additive did not improve, but slightly impair device performance.

22 (a) T. Xu and L. Yu, *Mater. Today*, 2014, **17**, 11; (b) Y. Liang, D. Feng, Y. Wu, S.-T. Tsai, G. Li, C. Ray and L. Yu, *J. Am. Chem. Soc.*, 2009, **131**, 7792; (c) L. Ye, S. Zhang, L. Huo, M. Zhang and J. Hou, *Acc. Chem. Res.*, 2014, **47**, 1595.

23 (a) K. Graham, C. Cabanetos, J. P. Jahnke, M. N. Idso, A. E. Labban, G. O. N. Ndjawa, T. Heumueller, K. Vandewal, A. Salleo, B. F. Chmelka, A. Amassian, P. M. Beaujuge and M. D. McGehee, *J. Am. Chem. Soc.*, 2014, **136**, 9608; (b) P. M. Beaujuge and J. M. J. Fréchet, *J. Am. Chem. Soc.*, 2011, **133**, 20009.

24 In order to facilitate the analysis, $PC_{61}BM$ with few isomers was applied for solid-state 2D NMR measurements.

25 H. Zhou, L. Yang and W. You, *Macromolecules*, 2012, **45**, 607.

26 (a) L. Dou, J. You, J. Yang, C.-C. Chen, Y. He, S. Murase, T. Moriarty, K. Emery, G. Li and Y. Yang, *Nature Mater.*, 2012, **6**, 180; (b) T. Ameri, N. Li and C. J. Brabec, *Energy Environ. Sci.*, 2013, **6**, 2390.

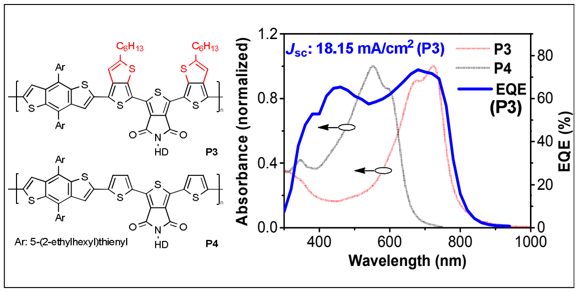
C_6H_{13}
C_6H_{13}
Ar
S
Ar
n
O
N
O
HD
P3
P4
Ar: 5-(2-ethylhexyl)thienyl
J_{sc}: 18.15 mA/cm^2 (P3)
P3
P4
EQE
(P3)
Absorbance (normalized)
EQE (%)
Wavelength (nm)
0.0
0.4
0.8
1.2
400
600
800
1000
0
20
40
60
80